

Green Synthesis of Silver Nanoparticles Using Extract of *Jasminum officinale* L. Leaves and Evaluation of Cytotoxic Activity Towards Bladder (5637) and Breast Cancer (MCF-7) Cell Lines

This article was published in the following Dove Press journal:
International Journal of Nanomedicine

Seham Elhawary¹
Hala EL-Hefnawy¹
Fatma Alzahraa Mokhtar¹
Mansour Sobeh²
Eman Mostafa³
Samir Osman^{4,*}
Mohamed El-Raey^{5,*}

¹Department of Pharmacognosy, Faculty of Pharmacy, Cairo University, Cairo, Egypt; ²Agro-BioSciences Research Division, Mohammed VI Polytechnic University, Ben-Guerir 43150, Morocco; ³Department of Pharmacognosy, Faculty of Pharmacy, October University for Modern Sciences and Arts (MSA), 6 October City, Giza, Egypt; ⁴Department of Pharmacognosy, Faculty of Pharmacy, Oct. 6 University, Giza, Egypt; ⁵Phytochemistry and Plant Systematic Department, National Research Centre, Dokki, Cairo, Egypt

*These authors contributed equally to this work

Introduction: *Jasminum officinale* L. is a very important medicinal and industrial flowering aromatic plant.

Methods: The present study deals with *Jasminum officinale* L. leaves extract (JOLE) as a reducing and capping agent for the synthesis of silver nanoparticles (AgNPs) by the green pathway. Phenolic profile of the extract was evaluated using HPLC-PDA/MS/MS technique. *Jasminum officinale* L. leaves extract silver nanoparticles (JOLE-AgNPs) were characterized by ultraviolet light (UV), Fourier transform infrared spectroscopy (FTIR), transmission electron microscopy (TEM), zeta potential and X-ray diffraction (XRD). JOLE-AgNPs were examined for their cytotoxic activities by neutral red uptake assay (NRU) against bladder (5637) and breast cancer (MCF-7) cell lines.

Results: HPLC-PDA/MS/MS tentatively identified 51 compounds of different chemical classes. UV spectra showed absorption peak at $\lambda_{max} = 363$ nm. The biosynthesized AgNPs were predominantly spherical in shape with an average size of 9.22 nm by TEM. The face centered cubic (fcc) nature of silver nanoparticles was proved by XRD diffractogram. JOLE-AgNPs exhibited high cytotoxic activity against 5637 and MCF-7 cell lines compared to the cytotoxic activities of JOLE with IC_{50} of 13.09 μ g/mL and 9.3 μ g/mL, respectively.

Discussion: The silver nanoparticles formed by *Jasminum officinale* L. showed high cytotoxic activities against MCF-7 and 5637 cell lines and can be introduced as a new alternative cytotoxic medication.

Keywords: silver nanoparticles, HPLC-PDA/MS/MS, cytotoxic, *Jasminum*, bladder cancer, breast cancer

Introduction

Nanotechnology is a progressive science of applying nanoparticles in different sectors of technology, it has revolutionized many sectors of technology, medicine and industry, particularly the pharmaceutical and energy industry, food safety and environmental sciences, among many others.¹

The application of nanotechnology in medicine depends on the natural scale of biological phenomena to produce precise means of disease prevention, diagnosis and treatment.²

Formation of metal nanoparticles with optimum physical and chemical characters was the main goal of different research groups in the last few years. Formation

Correspondence: Fatma Alzahraa Mokhtar
Department of Pharmacognosy, Faculty of Pharmacy, Cairo University, Cairo 12412, Egypt
Tel +201113154863
Email drfatmaalzahraa1950@gmail.com

of metal nanoparticles through chemical reactions, thermal decomposition or microwave-irradiation lead to the formation of toxic waste products and involves toxic chemicals; so biogenerations of metal nanoparticles through natural mechanisms using bacterial, fungal, or plant extracts are favorable methods to form safe clean and bio-friendly nanoparticles. Reduction of silver nitrate by plant extracts to form silver nanoparticles is a safe, clean, and rapid technique. The plant extract acts as a safe natural capping, reducing and stabilizing agent with no thermal or chemical hazards, many plant extracts were used for the formation of silver nanoparticles.³

Formation of nanoparticles may be a glimmer of hope for the production of vaccines and treatments that are inefficient and effective for many intractable viral epidemic diseases such as Covid-19.⁴

Jasminum officinale L. belongs to the family Oleaceae and known as true jasmine, common jasmine, or poet jasmine and is a species of flowering plant with very pleasant aroma.⁵ It is a well-known aromatic medicinal and industrial plant containing alkaloids, sesquiterpenes, secoiridoids and flavonoids.^{6,7} *Jasminum officinale* showed several pharmacological activities as antimicrobial, antiviral, wound healing promoter and antispasmodic agent,^{8–11} in addition to cytotoxic activities.¹²

Green synthesized silver nanoparticles differ in their biological activities according to the capping agent (plant extract) composition; silver nanoparticles (AgNPs) of *Acalypha wilkesiana* flowers exhibited potent cytotoxic activity against MCF-7 (breast carcinoma) and PC-3 (prostate carcinoma) cell lines, while the AgNPs of *Caesalpinia gilliesii* against MCF-7 showed moderate anticancer activity.^{13,14} Therefore, detection of plant chemical composition tentatively by HPLC-PDA/MS/MS can identify the possible major molecular structures that play a role in green nanoparticles formation as mentioned in our previous study on other *Jasminum* species (*Jasminum sambac*).¹⁵

In the present study, *Jasminum officinale* L. leaf extract (JOLE) was used for the biosynthesis of silver nanoparticles (AgNPs). The synthesized AgNPs using JOLE (JOLE-AgNPs) were characterized through UV-visible spectroscopy followed by X-ray diffraction (XRD), TEM (transmission electron microscopy), zeta potential and FTIR (Fourier transform infrared spectroscopy). JOLE and JOLE-AgNPs were examined for their cytotoxic activities by neutral red assay against two cell lines; breast (MCF-7) and bladder (5637) cancer cell lines.

Investigation of JOLE secondary metabolites by HPLC-PDA/MS/MS was performed to evaluate the role of the plant constituents that affect the nanoparticles formation.

This study was designed to evaluate the ability of *Jasminum officinale* leaves extract to act as a reducing agent on AgNO₃ to form ecofriendly, small particles, clean silver nanoparticles, and study the enhancement of the cytotoxic activity of the formed nanoparticles.

Materials and Methods

Preparation of Extract

Jasminum officinale L. leaves powder, prepared from the dried fine ground leaves, collected from Keram farms, El-Behaira Government, Egypt, and used for the biosynthesis of AgNPs. The plant was authenticated by Dr. Mohammed El Gebaly (consultant Botanist-Orman Garden), voucher specimen (# 37116.6) was kept at the Department of Pharmacognosy, Faculty of Pharmacy, Cairo University.

Powdered leaves (10 g) were mixed in 90 mL of distilled water and incubated at room temperature for 24 h. The extract was filtered and centrifuged for 40 min at 4000 rpm. The supernatant was used for AgNPs biosynthesis and stored at 4 °C for further use.

Identification of Extract Constituents

The aqueous extract of leaves of *Jasminum officinale* L. was used for HPLC-PDA-MS/MS. For MS analysis, LCQ-Duo ion trap having a Thermo Quest ESI source was used,¹⁶ Xcalibur software (Xcalibur™ 2.0.7, Thermo Scientific, Waltham, MA, USA) was used for system control. MS operating parameters in the negative ion mode were used.¹⁷

Synthesis of Silver Nanoparticles

AgNPs were synthesized according to the following protocol: 1 mM aqueous solution of silver nitrate (AgNO₃) in dist. H₂O was prepared and kept in a cool and dark place to be used for the synthesis of silver nanoparticles. 10 mL of the extract of leaves of JOLE into 90 mL of aqueous solution of 1 mM silver nitrate for reduction of Ag⁺ ions to nano silver particles in a molar concentration of (1.7 mg of silver nitrate: 1.2 mg extract) and incubated at room temperature in a dark place (for 24 h). The formation of a yellowish brown solution was the indication for the formation of silver nanoparticles.¹⁸ The formed solution was used directly for TEM, HR-TEM and UV quantifications then centrifugation at 4000 rpm for 30 minutes,

followed by a series of washes with distilled water and filtration to obtain pure AgNPs. The pure AgNPs were used for FTIR, XRD, Zeta potential and cytotoxicity study.^{19–21}

Characterization of Silver Nanoparticles

UV-Spectroscopy

The bioreduction of AgNPs was confirmed by subjecting diluted aliquots of the silver metallic NPs to UV-visible spectrophotometry (Model Shimadzu UV- 2450, Japan) in the range of 300–500 nm the UV-visible results were a confirmation tool for the formation of silver nanoparticles.²²

Fourier Transform Infrared Spectroscopy (FTIR)

The different functional groups of the prepared nanomaterials in the range of 4000–400 cm^{-1} were measured by a Fourier transform infrared spectroscopy (FTIR) 6100 spectrometer (Jasco, Japan).

X-Ray Diffraction (XRD)

The XRD analysis was performed as a surface chemical analysis tool for characterization of metal nanoparticles.²³ XRD was performed using a XPERT-PRO-PANalytical Powder Diffractometer (PANalytical B.V., Almelo, The Netherlands) using monochromatic radiation source $\text{Cu K}\alpha$ radiation ($\theta = 1.5406 \text{ \AA}$) at a voltage of 45 kV and current of 30 mA at room temperature. The instrumental data for the silver nano powder were operated over a 2θ range of 4.01° – 79.99° .

Transmission Electron Microscope (TEM) and High Resolution TEM (HR-TEM)

The morphology of the particles (shape and dimensions) was examined by transmission electron microscope (TEM). (JEOL-JEM-1011, Japan) and high resolution electron microscope (HR-TEM) at 200 kV (JEOL-JEM-2100, Japan). Sample for TEM and HR-TEM analysis were prepared by placing 3 mL of the sample on the copper grid and kept for drying at room temperature for 15 min.

Zeta Potential and Dynamic Light Scattering (DLS)

Particle size, homogeneity of distribution and zeta potentials of nanoparticles were determined using Zeta sizer Nano ZN (Malvern Panalytical Ltd, United Kingdom). Before the measurements, dilution of an aliquot of nanoparticles with ultra purified water, then sonication for 15 min was performed.

Cytotoxicity Assay

MCF-7, 5637 and HaCaT cells were obtained from CLS Cell Lines Service (Eppelheim, Germany). Cells were cultured in RPMI 1640 medium (BioWhittaker, Lonza, Belgium) supplemented with 8% fetal bovine serum (Sigma Aldrich, Germany) and antibiotics (100 U/mL penicillin/100 $\mu\text{g/mL}$ streptomycin; Sigma Aldrich, Germany) at 95% humidity, 5% CO_2 and 37.5°C . MCF-7, 5637 and HaCaT cells were sub-cultured twice a week and regularly tested for mycoplasma contamination. Cell viability (cytotoxicity) of test samples was investigated on the cell lines using the neutral red uptake (NRU) assay.

Statistical Analysis

Calculations of the arithmetic means and the standard deviation of all tests were carried out using the software program Microsoft Excel 2007. Statistical analysis was performed using GraphPad Prism version 5.01. One-way ANOVA, followed by the Tukey-posthoc-test, was used to determine the statistical significance in comparison to the reference standard. All data are presented as mean \pm S.D. values of three independent determinations. The p -value ≤ 0.05 was statistically significant.

Results

Phenolic Profiling of JOLE

By the result of HPLC-PDA/MS/MS technique, the phenolic composition of the extract was investigated and led to the tentative identification of 51 compounds of different classes of secondary metabolites; mainly simple phenolic compounds, secoiridoid glycosides, flavonoid glycosides and lignans (Figure 1, Table 1).

Simple Phenolic Compounds

The free phenylethanoids, phenolic acids and their glycosides were the major simple phenolic compounds identified in the JOLE, the identified phenyl ethanoids are salidroside hexoside (1), hydroxytyrosol hexoside (2), salidroside (3), hydroxytyrosol (4) and tyrosol (7). The identified phenolic acids are: protocatechuic acid (5), chlorogenic acid (6), *p*-hydroxy benzoic acid (8), *p*-coumaroyl hexoside (9), caffeoyl quinic acid (10), caftaric acid hexoside (12), dihydrosinapic acid hexoside (13), syringic acid hexoside (14), syringic acid (15), *p*-coumaric acid (16) and rosmarinic acid (17), as mentioned in Table 1.

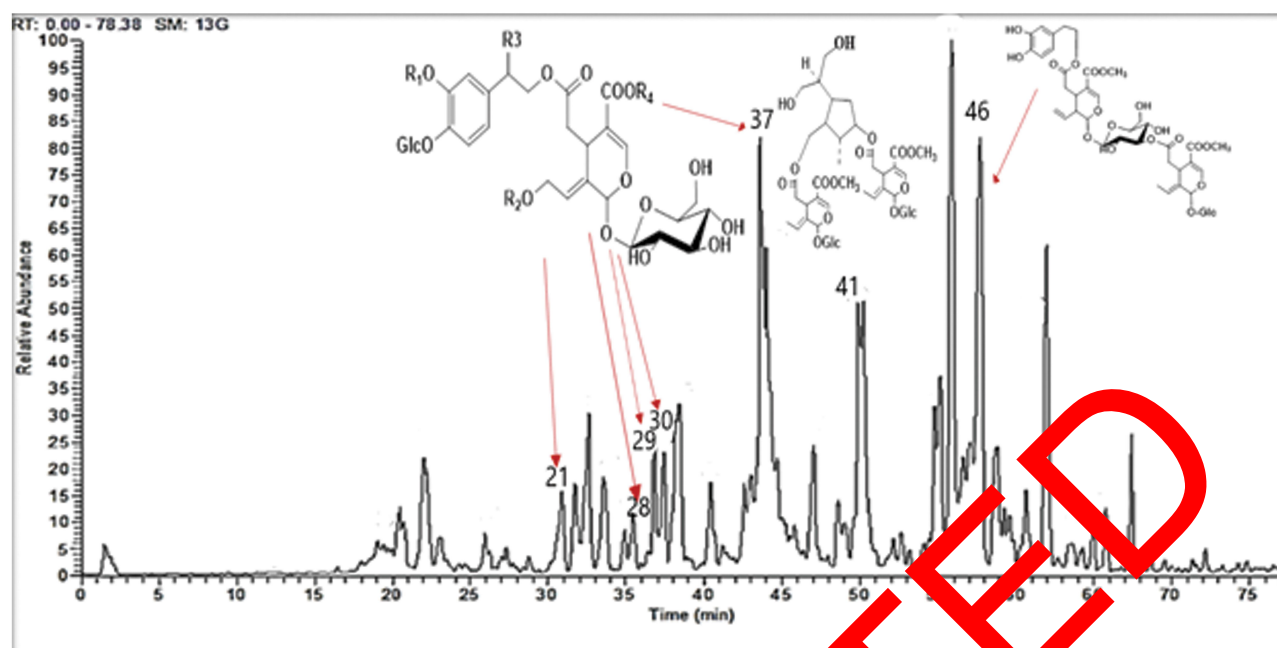


Figure I Total ion chromatogram of *J. officinale* leaves extract by HPLC-PDA-MS/MS in negative ion mode, red arrows point to the major identified secoiridoids.

Flavonoid Glycosides

The chromatographic analysis of flavonoids present in the JOLE by HPLC-PDA-MS/MS led to the identification of mono- and diglycosides. The identified flavonoids are derivatives of quercetin, kaempferol, and isorhamnetin. Quercetin derivatives are supported by the presence of base peak ions of $[M-H]^- = 301$ and a fragment ion $m/z = 179$, with UV absorbance range of $\lambda_{max} = 255-267$ nm. Quercetin diglycosides are; quercetin deoxyhexosyl hexoside (18) with a molecular ion peak of $[M-H]^- = 609$ and base peaks $[M-H]^- = 463$ and 301, quercetin hexosyl deoxyhexoside (23) with a molecular ion peak of $[M-H]^- = 609$ and base peaks $[M-H]^- = 447$ and 301.

Kaempferol glycosides are supported by the presence of base peak ions of $[M-H]^- = 285$ and a fragment ion $m/z = 179$, with UV absorbance range of $\lambda_{max} = (338-347)$ nm. Kaempferol deoxyhexosyl hexoside (22) with a molecular ion peak of $[M-H]^- = 593$ and base peaks $[M-H]^- = 447$ and 285 and Kaempferol hexoside (26) with a molecular ion peak of $[M-H]^- = 447$.

Isorhamnetin hexosyl deoxyhexoside (27) was supported by the presence of base peak ions of $[M-H]^- = 315$ and a fragment ion $m/z = 179$, with UV absorbance of $\lambda_{max} = 333$ nm.

Secoiridoids

The analysis confirmed the presence of 26 secoiridoids; the most identified secoiridoids are monomeric

secoiridoids conjugated to phenolic compounds (tyrosol, hydroxytyrosol and caffeic acid). Secoiridoid glycosides attached to tyrosol; demethyl ligstroside (28) and ligstroside (29) and oleuropein hexoside (30) with molecular ion peak at $[M-H]^- = 509$ and 609, respectively, the secoiridoids attached to hydroxytyrosol; demethyl oleuropein (21), oleuropein dihexoside (29), oleuropein (37) methoxy oleuropein (39) and oleuropein aglycone (45) with the presence of the characteristic molecular ion peaks at $[M-H]^- = 307$, the secoiridoids attached to caffeic acid; jaslanceoside D (31), jaslanceoside F (33), caffeoyl jasnervoside B (42).

Secoiridoids lactones are monomeric secoiridoids identified in the chromatogram; jasmolactone B (36) with a molecular ion peak of $[M-H]^- = 393$ and base peaks $[M-H]^- = 375$ and 343.

Dimeric Secoiridoids

Dimeric secoiridoids are iridoids characterized by the presence of two molecules or oleoside or oleoside methyl ester; that is represented in the chromatograms by the base peaks $[M-H]^- = 389$ and 403 for oleoside and oleoside methyl esters; respectively, with UV absorbance range of $\lambda_{max} = (222-236)$ nm. The dimeric secoiridoids identified in the extract are six compounds; jasnervoside A (34), molihauseide A (41), jaspolyoside (46), jaspolyanoside (47), jaspogeranoside B (48) and jasnervoside D (51), with molecular ion peaks of $[M-H]^- = 1171, 975, 925, 909, 945,$ and 1079; respectively.

Table I Tentative Identification of Chemical Profile of Aqueous Extract of *J. officinale* Leaves by HPLC-PDA-MS/MS in the Negative Ion Mode

No	R _t (min)	[M-H]	MS/MS	UV	Identified Compound	Reference
1	9.74	461	299	277	salidroside hexoside	[27]
2	10.22	315	153,137	276	hydroxytyrosol hexoside	[28]
3	10.64	299	137	276	salidroside	[27]
4	11.27	153	137	276	hydroxytyrosol	[28]
5	12.22	153	109	285	protocatechuic acid	[29]
6	12.92	353	191, 179	218,298	chlorogenic acid	[30]
7	13.7	137	119, 93	277	tyrosol	[31]
8	15.43	137	93	280,310	<i>p</i> -hydroxy benzoic acid	[32]
9	15.71	325	163	288	<i>p</i> -coumaroyl hexoside	[33]
10	18.63	353	191, 179	n.d.	caffeoyl quinic acid	[33]
11	19.05	565	403	229	oleoside methyl ester hexoside	[34]
12	20.09	473	311, 179	296,312	caftaric acid hexoside	[35]
13	22.65	387	225, 223	290	dihydrosinapic acid hexoside	[36]
14	23.47	359	197, 154	295	syringic acid hexoside	[37]
15	24.72	197	171, 153	283	syringic acid	[37]
16	25.06	163	119	280	<i>p</i> -coumaric acid	[38]
17	25.62	359	197,179,161	312,360	isomarinic acid	[39]
18	27.76	609	463, 301	256,358	quercetin deoxyhexosyl hexoside	[40]
19	27.83	537	447,375,179	226,286	hydroxy ptericresinol hexoside	[41]
20	28.92	717	555	222,276	hydroxy oleuropein hexoside	[42]
21	30.59	525	363, 307	222,276	demethyl oleuropein	[43]
22	31.27	593	447, 285	256,347	kaempferol deoxyhexosyl hexoside	[44]
23	32.49	609	447, 301	256,356	quercetin hexosyl deoxyhexoside	[45]
24	33.38	463	301	256,356	quercetin hexoside	[40]
25	33.57	697	535, 373,191	n.d.	hydroxypinoresinol dihexoside	[46]
26	34.30	447	285	256,356	kaempferol hexoside	[47]
27	35.26	623	461, 315	255,333	isorhamnetin hexosyl deoxyhexoside	[48]
28	36.34	509	377, 233	232,377	demethyl ligstroside	[49]
29	36.99	863	701, 347	231,277	oleuropein dihexoside	[50]
30	38.34	685	523, 377,233	230,277	ligstroside hexoside	[33]
31	38.69	565	403, 385	233,278	jaslanceoside D	[51]
32	39.36	831	401, 383	233,279	jaslanceoside F	[51]
33	40.66	533	391, 221	232	shanzhiside hexoside	[52]
34	41.09	1171	1009, 403	231	jasnervoside A	[53]
35	41.5	653	421	218,288	methoxy verbascoside	[54]
36	44.03	533	375, 343	232	jasmolactone B	[55]
37	44.11	539	377, 307	231,277	oleuropein	[56]
38	44.5	535	389,163	230,282	coumaroyl oleoside	[57]
39	46.91	509	537,389	232,278	methoxy oleuropein	[43]
40	47.86	627	465, 301	280,348	quercetin coumaroyl hexoside	[58]
41	48.1	975	813, 539,403	233	molihauseide A	[59]
42	48.68	1077	909,389,179	231,282	caffeoyl jasnervoside B	[60]
43	53.5	941	909, 555	229	jaspogeroside A	[61]
44	54.80	925	539,403	231	isojaspolyanoside B	[62]
45	55.83	377	307, 223	231,277	oleuropein aglycone	[63]
46	57.63	925	893,539,521	229	jaspolyoside	[64]
47	61.77	909	523,223	229	jaspolyanoside	[65]
48	63.15	945	727,595,389	230	jaspogeroside B	[61]
49	65.74	571	539	228	deacyl jaspofoliamoside E	[66]
50	68.05	957	571,223	230	jasamplexoside B	[67]
51	71.29	1079	833, 539	231	jasnervoside D	[68]

Abbreviations: R_t, retention time; n.d., not detected.

Nanoparticles Characterization

Physical Observation

The synthesis was investigated at initial silver ion concentration of 1 mM. In a typical experiment, 90 mL of 1 mM silver nitrate was reacted with 10 mL of JOLE. After 4 h, the formation of Ag nanoparticles was observed and detected by the appearance of dark brown coloration.

UV-Spectroscopy

UV-spectroscopy is a simple, selective and accurate technique for monitoring the synthesis and stability of AgNPs. AgNPs exhibit particular and unique optical characteristics, that allow them to powerfully interact with certain light wavelengths. The free electrons give rise to a surface plasmon resonance (SPR) absorption band due to the collective oscillation of electrons of AgNPs. The absorption of AgNPs depends on the chemical surroundings, particle's dimensions and particle size.

The appearance of the new broad absorption peak at 363 nm after 4 h indicated that the formation of AgNPs started within 4 h after JOLE interact with Ag^+ ions. The formed peak at $\lambda_{\text{max}} = 363$ nm is evidence on the formation of aggregated and mostly spherical NPs, so UV spectroscopy is an appropriate technique to inform the formation of AgNPs.²⁴ (Figure 2).

Fourier Transform Infrared Spectroscopy (FTIR)

The FTIR spectroscopy analysis was performed to identify the phytoconstituents possible biomolecules of JOLE that

are responsible for the synthesis of AgNPs. The peaks near 3390, 2921 and 1618 cm^{-1} (Figure 3A) could be due to the O-H, aliphatic C-H and C=O stretching vibration of secoiridoids/flavonoids/phenolic acids. The peak at 1410 cm^{-1} corresponds to polyphenols and affirm the existence of an aromatic ring, while the signals at 1044 cm^{-1} were assigned for the C-O-C and secondary OH groups of JOLE. There was a deviation of a signal detected for AgNPs at 3390 and 1618 cm^{-1} (Figure 3B), it suggests that the O-H and C=O groups were responsible for the reduction of AgNO_3 and formation of AgNPs.

TEM and HR-TEM

The formed JOLE-AgNPs after 48 h were predominantly of spherical shape, with an average size of 9.2 nm (Figure 4).

Zeta Potential and Dynamic Light Scattering (DLS)

Dynamic light scattering measures the hydrodynamic size and the ligand shell of the formed nanoparticles, the size is different from the TEM and HR-TEM where only the metallic core is measured. DLS of JOLE-AgNPs is 87.6 ± 2.11 nm and homogenous distribution of the formed nanoparticles with (polydispersity index: 0.312 ± 0.032). The zeta potential is a measure of nanoparticles stability through measuring of the surface charge potential in aqueous suspensions. Zeta potential values of AgNPs were measured to be -25.5 ± 0.7 mV (Figure 5). The produced nanoparticles had a negative charge on their surface, which indicates a high stability.²⁵

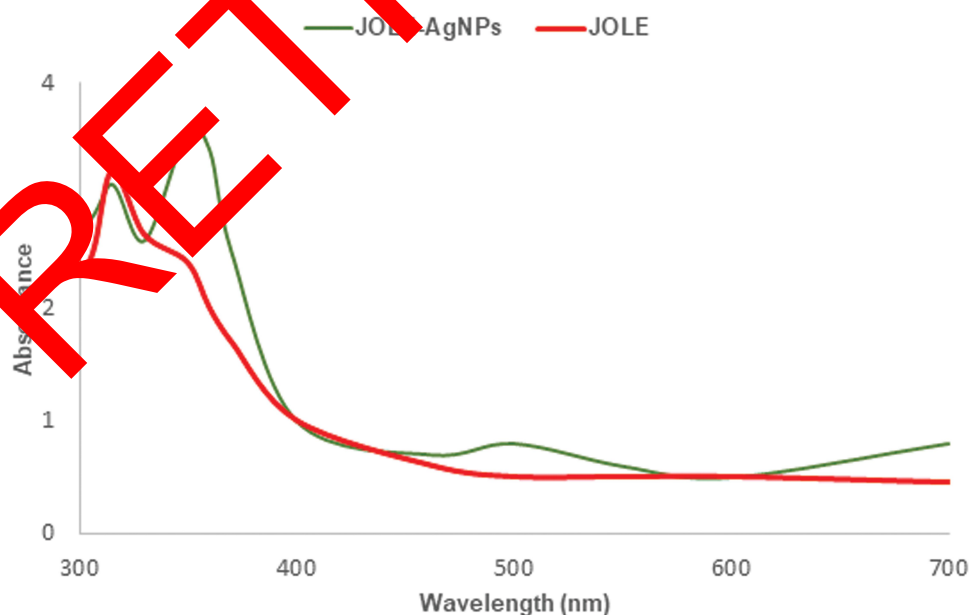


Figure 2 UV absorbance spectrum of JOLE(*Jasminum officinale* leaves extract) and JOLE-AgNPs(*Jasminum officinale* leaves extract mediated silver nanoparticles).

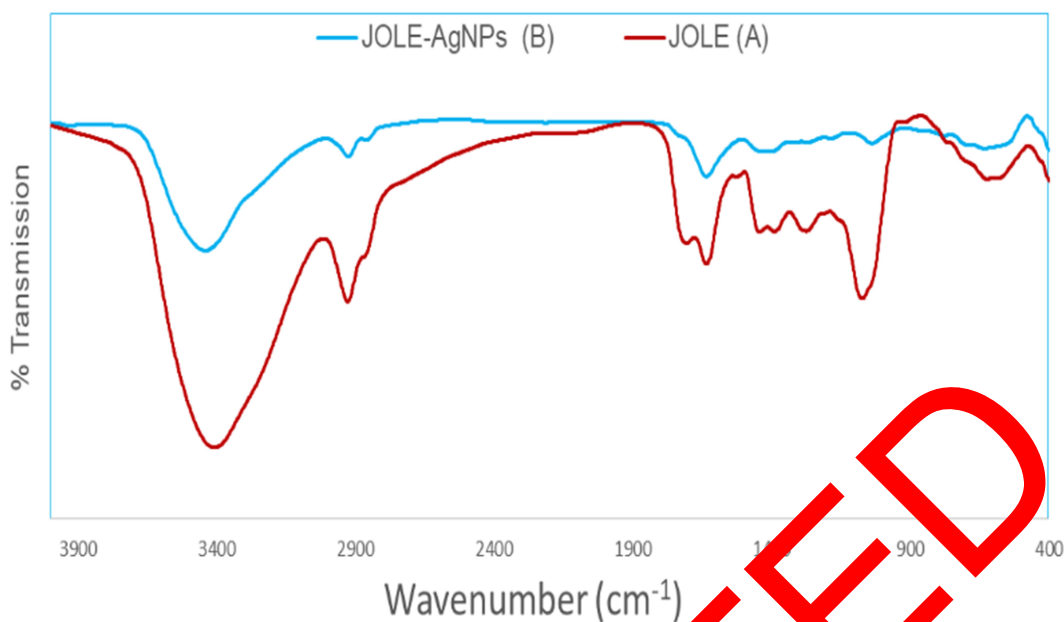


Figure 3 Fourier transform infrared spectroscopy (FTIR) of (A): (JOLE), *J. officinale* leaves extract; (B): *J. officinale* leaves extract-AgNPs, (JOLE-AgNPs) with similarities suggesting the presence of the total extract with the formed silver nanoparticles, indicating the capping function of the extract.

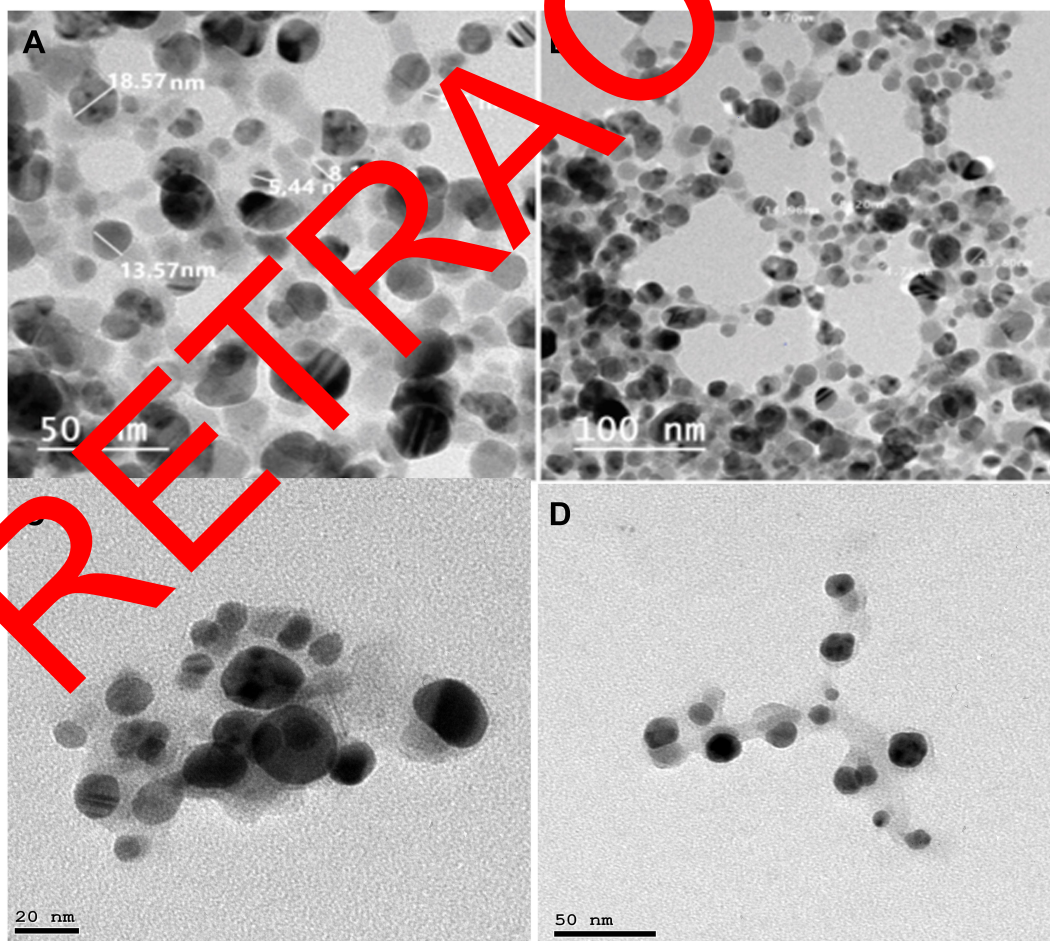


Figure 4 (A, B) TEM images, (C, D) HR-TEM of JOLE-AgNPs (*Jasminum officinale* leaves extract mediated silver nanoparticles) at different scales.

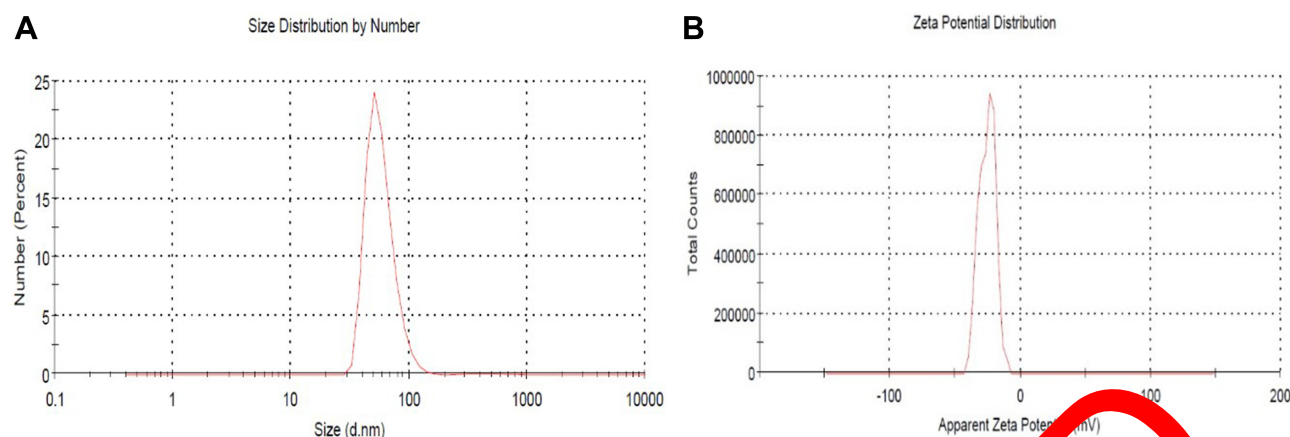


Figure 5 (A) Zeta potential and (B) Dynamic light scattering (DLS) of JOLE-AgNPs (*Jasminum officinale* leaves extract mediated silver nanoparticles).

X-Ray Diffraction (XRD)

The diffractogram of JOLE-AgNPs, the obtained diffraction silver nano peaks at 38.60° , 44.16° , 64.52° and 77.34° are respectively assigned to (111), (200), (220) and (311) planes (Figure 6), consistent with the face cubic center (fcc) nature of silver nanoparticles. This corresponds to the Joint Committee on Powder Diffraction Standards-International Center for Diffraction Data No. 64-2663, indicating the crystalline nature of the biosynthesized silver nanoparticles as confirmed by the corresponding peaks with respect to Bragg's model of diffraction. The results are consistent with the reference data of silver nanoparticle formation.²⁶

Cytotoxicity

The bladder cancer (5637) and breast cancer (MCF-7) cell lines, were exposed to (JOLE) and (JOLE-AgNPs),

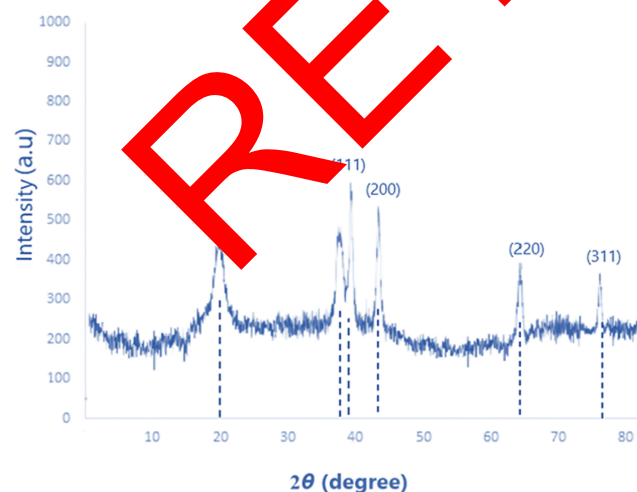


Figure 6 X-ray diffraction pattern of JOLE-AgNPs (*Jasminum officinale* leaves extract mediated silver nanoparticles).

and the cytotoxicity determined using the NRU assay were examined for their cytotoxic activities by neutral red assay at the concentration of 10–280 $\mu\text{g}/\mu\text{L}$ for 24 h towards two cell lines: bladder cancer (5637) and breast cancer (MCF-7) using propidium reference standard and compared to normal keratinocyte cells (HaCaT). NRU results have shown that AgNPs could significantly induce cytotoxicity in bladder cancer (5637) and breast cancer (MCF-7) cell lines, in a dose-dependent manner. Data analysis of the cytotoxicity assay has shown that the IC_{50} values of (JOLE-AgNPs) against the 5637 and MCF-7 cell lines and HaCaT, were 13.1 $\mu\text{g}/\mu\text{L}$, 9.3 $\mu\text{g}/\mu\text{L}$ and 183.8 $\mu\text{g}/\mu\text{L}$; respectively after the incubation periods ($P < 0.05$). Whereas the IC_{50} values of JOLE shows 28.8 $\mu\text{g}/\mu\text{L}$, 40.0 $\mu\text{g}/\mu\text{L}$ and 477.4 $\mu\text{g}/\mu\text{L}$ against the 5637 and MCF-7 cancer cell lines and HaCaT, respectively, after the incubation time. (Figure 7). The cytotoxicity results indicated the improvement of the cytotoxicity characteristics of leaves extract of *Jasminum officinale* upon formation of its corresponding AgNPs, especially towards the 5637, and MCF-7 cancer cell lines with very low toxicity towards normal cell line HaCaT.

Conclusion

Medicinal plants, namely, aqueous extracts of fresh leaves of *Jasminum officinale* L. can be used as bioreduction agents to produce clean, inexpensive, ecofriendly silver nanoparticles and a safe method that has not used any toxic substance and consequently does not have side effects. Nanoparticles formation was observed by the color change of *J. officinale* extract into a brownish-yellow. Color changes that occur indicate that AgNO_3 was reduced and Ag nanoparticles have been formed.

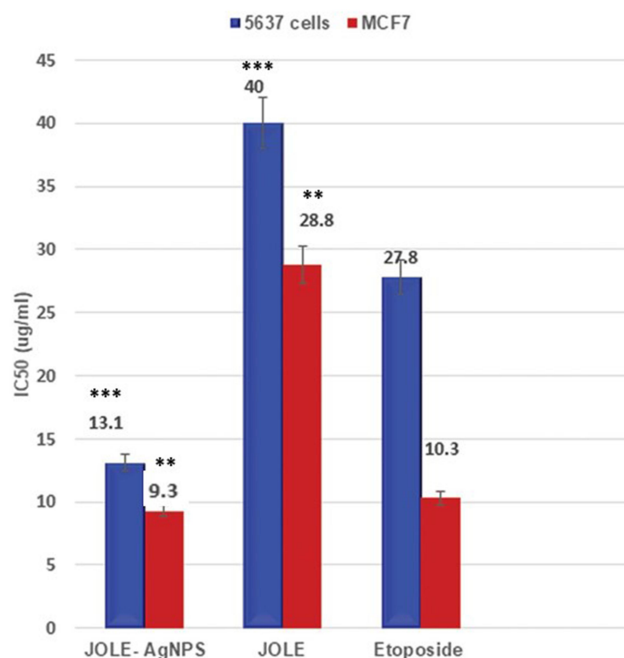


Figure 7 IC₅₀ of JOLE and JOLE-AgNPs against 5637 bladder cancer cell line and MCF-7 breast cancer cell line in comparison to Etoposide as a reference standard. Data were analyzed using one-way ANOVA followed by Tukey's test. Each value represents the mean \pm S.D. for n = 3. Values are compared to reference standard, **p<0.01, ***p<0.001.

HPLC-PDA/MS/MS tentatively identified 51 compounds of different classes; secoiridoid glycosides as a major class of compounds, phenolic acids and flavonoids. Formation of silver nanoparticles were proved physically through color change of the extract solution to a brownish-yellow color. UV spectra showed a broad absorption peak at $\lambda_{\text{max}} = 223$ nm, which represents spherical and aggregated NPs. The biosynthesized AgNPs were predominantly spherical in shape with an average size of 9.22 nm by TEM. The face cubic center (fcc) nature of silver nanoparticles was proved by XRD diffractogram. Zeta potential values of AgNPs were measured -25.5 ± 0.7 silver nanoparticles proved the stability of these silver nanoparticles with JOLE-AgNPs exhibiting high cytotoxic activity towards 5637 and MCF-7 cell lines compared to the cytotoxic activities of JOLE with IC₅₀ of 13.09 $\mu\text{g/mL}$ and 9.3 $\mu\text{g/mL}$, respectively. The former silver nanoparticles showed high cytotoxic activities and can be introduced as a new alternative cytotoxic medication.

Acknowledgment

The authors would like to thank Professor Michael Wink, Heidelberg University, Germany, for providing the laboratory facilities to carry out the HPLC-PDA-MS/MS analysis.

Funding

This research did not receive any specific grant from funding agencies in the public, commercial, or not-for-profit sectors.

Disclosure

The authors report no conflicts of interest in this work and there has been no significant financial support for this work that could have influenced its outcome.

References

1. Wolf EL. Nanophysics and nanotechnology. *Weinheim*. 2004;24: 452.
2. Emerich DF, Thanos CA. Nanotechnology and medicine. *Expert Opin Biol Ther*. 2007;7(4):655–663. doi:10.1080/14712598.3.4.655
3. Fedlheim DL, et al. *Metal Nanoparticles: Synthesis, Characterization, and Applications*. CRC press; 2001.
4. Hu TY, Friedman M, Williams J. Insights from nanomedicine into chloroquine efficacy against COVID-19. *Nat Nanotechnol*. 2020;1–3.
5. Krishnaswamy V, Raman V. Cytogenetical studies of the Indian Jasmines. I. *Ind J Bot Soc*. 1948;27:77–83.
6. Gao G, Yin Z, Li Y, Li H. Iridoid glycosides from buds of *Jasminum officinale* L. var. *grandiflorum*. *Yao Xue Xue Bao*. 2011; 46:1221–1224.
7. Ali JK. Study of phenolic compound of some leaves of species of genus *L. Jasminum* growing in Iraq. *Al-Qadisiyah J Pure Sci*. 2019;22:107–108.
8. Lis Balchin M, Hart S, Wan Hang L. Jasmine absolute (*Jasminum grandiflora* L.) and its mode of action on guinea-pig ileum in vitro. *Phytotherapy Res*. 2002;16:437–439.
9. Zhao G. Anti-hepatitis B Virus Activity of 8-epi-Kingside in *Jasminum officinale* var. *grandiflorum*. *Chin Herbal Med*. 2013;5: 53–57.
10. Nagarajappa AK, Pandya D, Ravi K. Role of free radicals and common antioxidants in oral health, an update. *J Adv Med Res*. 2015;1–12.
11. Hirapara H, Ghori V, Anovadiya A, Baxi S, Tripathi C. Effects of ethanolic extract of *Jasminum grandiflorum* Linn. flowers on wound healing in diabetic Wistar albino rats. *Avicenna J Phytomed*. 2017;7:401.
12. Rahman M, Khatun A, Khan S, Hossain F, Khan A. Phytochemical, cytotoxic and antibacterial activity of two medicinal plants of Bangladesh. *Pharmacologyonline*. 2014;1:3–10.
13. Emam M, El Raey MA, Eisa WH, et al. Green synthesis of silver nanoparticles from *Caesalpinia gilliesii* (Hook) leaves: antimicrobial activity and in vitro cytotoxic effect against BJ-1 and MCF-7 cells. *J App Pharm Sci*. 2017;7:226–233.
14. El Raey MA, El-Hagrassi AM, Osman AF, Darwish KM, Emam M. *Acalypha wilkesiana* flowers: phenolic profiling, cytotoxic activity of their biosynthesized silver nanoparticles and molecular docking study for its constituents as Topoisomerase-I inhibitors. *Biocatalysis Agr Biotech*. 2019;20:101243. doi:10.1016/j.bcab.2019.101243
15. El-Hawary SS, El-Hefnawy HM, Osman SM, Mostafa ES, Mokhtar F, El-Raey M. CHEMICAL PROFILE OF TWO *JASMINUM* SAMBAC L. (AIT) CULTIVARS CULTIVATED IN EGYPT–THEIR MEDIATED SILVER NANOPARTICLES SYNTHESIS AND SELECTIVE CYTOTOXICITY. *International Journal of Applied Pharmaceutics*. 2019;154–164. doi:10.22159/ijap.2019v11i6.33646
16. Marrez DA, Abdelhamid AE, Darwesh OM. Eco-friendly cellulose acetate green synthesized silver nano-composite as antibacterial packaging system for food safety. *Food Packaging Shelf Life*. 2019;20:100302. doi:10.1016/j.fpsl.2019.100302

17. Sobeh M, Mahmoud MF, Abdelfattah MAO, Cheng H, El-Shazly AM, Wink M. A proanthocyanidin-rich extract from *Cassia abbreviata* exhibits antioxidant and hepatoprotective activities in vivo. *J Ethnopharmacol.* **2018**;213:38–47. doi:10.1016/j.jep.2017.11.007
18. Mulfinger L, Solomon SD, Bahadory M, Jeyarajasingam AV, Rutkowsky SA, Boritz C. Synthesis and study of silver nanoparticles. *Journal of Chemical Education.* **2007**;84(2):322. doi:10.1021/ed084p322
19. Edison TNJI, Atchudan R, Karthik N, Balaji J, Xiong D, Lee YR. Catalytic degradation of organic dyes using green synthesized N-doped carbon supported silver nanoparticles. *Fuel.* **2020**;280:118682. doi:10.1016/j.fuel.2020.118682
20. Edison TNJI, Atchudan R, Kamal C, Lee YR. *Caulerpa racemosa*: a marine green alga for eco-friendly synthesis of silver nanoparticles and its catalytic degradation of methylene blue. *Bioprocess and Biosystems Engineering.* **2016**;39(9):1401–1408. doi:10.1007/s00449-016-1616-7
21. Edison TNJI, Atchudan R, Lee YR. Optical sensor for dissolved ammonia through the green synthesis of silver nanoparticles by fruit extract of *Terminalia chebula*. *Journal of Cluster Science.* **2016**;27(2):683–690. doi:10.1007/s10876-016-0972-4
22. Aziz SB. Investigation of metallic silver nanoparticles through UV-Vis and optical micrograph techniques. *Int J Elect Sci.* **2017**;12:363–373. doi:10.20964/2017.01.22
23. Baer DR, Gaspar DJ, Nachimuthu P, Techane SD, Castner DG. Application of surface chemical analysis tools for characterization of nanoparticles. *Anal Bioanal Chem.* **2010**;396:983–1002.
24. Zou J, Xu Y, Hou B, Wu D, Sun Y. Controlled growth of silver nanoparticles in a hydrothermal process. *China Particuology.* **2007**;5(3):206–212. doi:10.1016/j.cpart.2007.03.006
25. Römer I, White TA, Baalousha M, Chipman K, Viant MR, Lead JR. Aggregation and dispersion of silver nanoparticles in exposure media for aquatic toxicity tests. *Journal of Chromatography A.* **2011**;1228(27):4226–4233. doi:10.1016/j.chroma.2011.03.034
26. Anandalakshmi K, Venugobal J, Ramasamy V. Characterization of silver nanoparticles by green synthesis method using *Pedicularis murex* leaf extract and their antibacterial activity. *Applied Nanoscience.* **2016**;6(3):399–408. doi:10.1007/s13204-015-0449-z
27. Zhao G, Yin Z, Dong J. A new secoiridoid from the flowers of *Jasminum officinale* L. var. *grandiflorum*. *Yao Xue Xue Bao.* **2008**;43:513–517.
28. De Leonardi A, Aretini A, Alfano M, Macciola V, Gnani G. Isolation of a hydroxytyrosol-rich extract from olive leaves (*Olea Europaea* L.) and evaluation of its antioxidant properties and bioactivity. *European Food Research and Technology.* **2008**;226(4):653–659. doi:10.1007/s00217-007-0574-3
29. Pandey KB, Rizvi SI. Plant polyphenols as dietary antioxidants in human health and disease. *Food Chem.* **2009**;2:270–278.
30. Clifford MN, Kondo T, Suruguch B, Kurihara N. Characterization by LC-MS of four new classes of chlorogenic acids in green coffee beans: dimethoxycinnamoylquinic acids, diferuloylquinic acids, caffeoyl-dimethoxycinnamoylquinic acids, and feruloyl-dimethoxycinnamoylquinic acids. *J Agric Food Chem.* **2006**;54:1957–1969.
31. Tuck KL, Freeman MP, Hayball PJ, Stretch GL, Stupans I. The in vivo fate of hydroxytyrosol and tyrosol, antioxidant phenolic constituents of olive oil, after intravenous and oral dosing of labeled compounds to rats. *J Nutr.* **2001**;131:1993–1996.
32. Dhakal RC, Rajbhandari M, Kalauni SK, Awale S, Gewali MB. Phytochemical Constituents of the Bark of *Vitex negundo* L. *J Nepal Chem Soc.* **2009**;23:89–92.
33. Sanz M, de Simón BF, Cadahía E, et al. LC-DAD/ESI-MS/MS study of phenolic compounds in ash (*Fraxinus excelsior* L. and *F. americana* L.) heartwood. Effect of toasting intensity at cooperage. *J Mass Spectrom.* **2012**;47:905–918.
34. Damtoft S, Franzky H, Jensen SR. Excelsioside, a secoiridoid glucoside from *Fraxinus excelsior*. *Phytochem.* **1992**;31:4197–4201.
35. Gu M, Wang X, Su Z, Ouyang F. One-step separation and purification of 3, 4-dihydroxyphenyllactic acid, salvianolic acid B and protocatechualdehyde from *Salvia miltiorrhiza* Bunge by high-speed counter-current chromatography. *J Chromatogr A.* **2007**;1140:107–111.
36. Nićiforović N, Abramović H. Sinapic acid and its derivatives: natural sources and bioactivity. *Compreh Rev Food Sci Food Safety.* **2014**;13:34–51.
37. Mattila P, Hellström J. Phenolic acids in potatoes, vegetables, and some of their products. *J Food Composition Analysis.* **2007**;20:152–160.
38. Cui Y, Li Q, Zhang M, et al. LC–MS Determination and Pharmacokinetics of p-Coumaric Acid in Rat Plasma after Oral Administration of p-Coumaric Acid and Freeze-Dried Red Wine. *J Agric Food Chem.* **2010**;58:12083–12088.
39. Pan J-Y, Cheng -Y-Y. Identification and quantification of absorbed and metabolic components in rat plasma after oral administration of ‘Shuangdan’ granule by HPLC–DAD/ESI-MS/MS. *J Pharm Biomed Anal.* **2006**;42:565–572.
40. Slatnar A, Mikulic-Petkovsek M, Stampar F, Veberic R, Solar A. Identification and quantification of phenolic compounds in kernels, oil and bagasse pellets of common walnut (*Juglans regia* L.). *Food Res Int.* **2015**;67:255–263.
41. Ricci A, Fiorentini A, Picotella S, D’Amorosa B, Pacifico S, Monaco P. Structural discrimination of isomeric tetrahydrofuran lignan glucosides by tandem mass spectrometry. *Rapid Commun Mass Spectrometry.* **2010**;24:979–985.
42. Shen Y-C, Lin C. Secoiridoid glycosides from *Jasminum multiflorum*. *Phytochem.* **1990**;22:2905–2912.
43. Tanahashi T, Takeraka Y, Nagakura N, Nishi T. Three secoiridoid glucosides from *Jasminum nudiflorum*. *J Nat Prod.* **1999**;62:1311–1315.
44. Belsels C, Gräter J, Esquivel P, Jiménez VM, Gänzle MG, Schieber A. Characterization of phenolic compounds in jocote (*Spondias purpurea* L.) peels by ultra high-performance liquid chromatography/electrospray ionization mass spectrometry. *Food Res Int.* **2012**;46:557–562.
45. Zhang Z, Bian B, Yang J, Tian X. Studies on chemical constituents in roots of *Jasminum sambac*. *Zhongguo Zhong Yao Za Zhi.* **2004**;29:237–239.
46. Eyles A, Jones W, Riedl K, et al. Comparative phloem chemistry of Manchurian (*Fraxinus mandshurica*) and two North American ash species (*Fraxinus americana* and *Fraxinus pennsylvanica*). *J Chem Ecol.* **2007**;33:1430–1448.
47. Yang J-H, Kondratyuk TP, Marler LE, et al. Isolation and evaluation of kaempferol glycosides from the fern *Neochlopteris palmatopoda*. *Phytochem.* **2010**;71:641–647.
48. Koike A, Barreira JC, Barros L, Santos-Buelga C, Villavicencio AL, Ferreira IC. Edible flowers of *Viola tricolor* L. as a new functional food: antioxidant activity, individual phenolics and effects of gamma and electron-beam irradiation. *Food Chem.* **2015**;179:6–14.
49. Shen Y-C, Lin S-L. New secoiridoid glucosides from *Jasminum lanceolarium*. *Planta Med.* **1996**;62:515–518.
50. Shen Y-C, Hsieh P-W. Four new secoiridoid glucosides from *Jasminum urophyllum*. *J Nat Prod.* **1997**;60:453–457.
51. Shen YC, Lin TT, Lu TY, Hung SE, Sheu JH. Secoiridoids Glycosides from *Jasminum amplexicaule*. *J Chin Chem Soc.* **1999**;46:197–200.
52. Ghule B, Palve S, Rathil L, Yeole P. Validated HPTLC method for simultaneous determination of shanzhiside methyl ester and barlerin in *Barleria prionitis*. *JPC.* **2012**;25:426–432.
53. Yin Y, Ying X, Luan H, et al. UPLC-DAD/Q-TOF-MS Based Ingredients Identification and Vasorelaxant Effect of Ethanol Extract of Jasmine Flower. *Evid Based Complementary Alternative Med.* **2014**, 2014.
54. Magiatis P, Mitaku S, Tsitsa E, Skaltsounis A, Harvala C. Verbascoside derivatives and iridoid glycosides from *Verbascum undulatum*. *Nat Prod Lett.* **1998**;12:111–115.

55. Shen Y-C, Chen C. Novel secoiridoid lactones from *Jasminum multiflorum*. *J Nat Prod*. 1989;52:1060–1070.
56. Amiot M-J, Fleuriot A, Macheix -J-J. Accumulation of oleuropein derivatives during olive maturation. *Phytochem*. 1989;28:67–69.
57. Cecchi L, Migliorini M, Cherubini C, et al. Phenolic profiles, oil amount and sugar content during olive ripening of three typical Tuscan cultivars to detect the best harvesting time for oil production. *Food Res Int*. 2013;54:1876–1884.
58. Imperato F. Kaempferol and Quercetin 3-O-(2", 3"-di-Op-coumaroyl)-glucosides from *Pteris vittata*. *Am Fern J*. 2003;157–160.
59. Zhang Y-J, Liu Y-Q, Pu X-Y, Yang C-R. Iridoidal glycosides from *Jasminum sambac*. *Phytochem*. 1995;38:899–903.
60. Bera P, Kotamreddy JNR, Samanta T, Maiti S, Mitra A. Inter-specific variation in headspace scent volatiles composition of four commercially cultivated jasmine flowers. *Nat Prod Res*. 2015;29:1328–1335.
61. Takenaka Y, Tanahashi T, Nagakura N. Five trimeric secoiridoid glucosides from *Jasminum polyanthum*. *Phytochem*. 1998;48:317–322.
62. Takenaka Y, Tanahashi T, Taguchi H, Nagakura N, Nishi T. Nine new secoiridoid glucosides from *Jasminum nudiflorum*. *Chem Pharm Bull*. 2002;50:384–389.
63. Impellizzeri D, Esposito E, Mazzon E, et al. Oleuropein aglycone, an olive oil compound, ameliorates development of arthritis caused by injection of collagen type II in mice. *J Pharmacol Exp Ther*. 2011;339:859–869.
64. Tanahashi T, Takenaka Y, Nagakura N. Two dimeric secoiridoid glucosides from *Jasminum polyanthum*. *Phytochem*. 1996;41:1341–1345.
65. Pérez-Bonilla M, Salido S, van Beek TA, et al. Isolation of antioxidative secoiridoids from olive wood (*Olea europaea* L.) guided by on-line HPLC–DAD–radical scavenging detection. *Food Chem*. 2011;124:36–41.
66. Yue Z, Qin H, Li Y, et al. Chemical constituents of the root of *Jasminum giraldii*. *Molecules*. 2013;18:4766–4775.
67. Tanahashi T, Shimada A, Nagakura N, Nayeshiro H, Jasamplexosides A. B and C: novel dimeric and trimeric secoiridoid glucosides from *Jasminum amplexicaule*. *Planta Med*. 2002;68:552–555.
68. Guo Z-Y. Antioxidant and anti-inflammatory effect of phenylpropenoid and secoiridoid glycosides from *Jasminum nervosum* stems, a Chinese folk medicine. *Phytochem*. 2014;106:124–133.

International Journal of Nanomedicine

Dovepress

Publish your work in this journal

The International Journal of Nanomedicine is an international, peer-reviewed journal focusing on the application of nanotechnology in diagnostics, therapeutics, and drug delivery systems throughout the biomedical field. This journal is indexed on PubMed Central, MedLine, CAS, SciSearch®, Current Contents®/Clinical Medicine,

Journal Citation Reports/Science Edition, EMBase, Scopus and the Elsevier Bibliographic databases. The manuscript management system is completely online and includes a very quick and fair peer-review system, which is all easy to use. Visit <http://www.dovepress.com/testimonials.php> to read real quotes from published authors.

Submit your manuscript here: <https://www.dovepress.com/international-journal-of-nanomedicine-journal>